THE ASTROPHYSICAL JOURNAL, 331:161–171, 1988 August 1

HARD X-RAY EMISSION FROM A TYPE 2 SEYFERT GALAXY (NGC 1068)

MARTIN ELVIS
Harvard-Smithsonian Center for Astrophysics

AND

A. LAWRENCE
Queen Mary College, London
Received 1987 September 24; accepted 1988 January 19

ABSTRACT

EXOSAT observations of the type 2 Seyfert galaxy NGC 1068 have detected a source in the 2–10 keV range with a flux density at 2 keV of 0.6 μJy. It has a flat ($\alpha_E = 0.62 \pm 0.25$) power-law spectrum similar to type 1 Seyferts. Combined with Low Energy *EXOSAT* filter data and *Einstein* IPC observations, these data show that spectral curvature is necessary, flattening the X-ray spectrum to high energies. The spectrum can be decomposed into two components: a steep low-energy part ($\alpha_E \approx 3.5$, $kT \approx 0.2$ keV) and a flat high-energy part ($\alpha_E \approx -0.3$ to 1.0). Any intrinsic absorption is small ($< 3 \times 10^{20}$ atoms cm^{-2}). There is no evidence for variability within or between any of the observations, which sample time scales from 30 minutes to 4 yr. These data support the "obscuration" model of type 2 Seyfert galaxies in which the nucleus is seen only in flux scattered from above a "wall" of material that completely blocks the direct view. The lack of absorption implies that electron scattering, rather than dust scattering is involved. Since the absorption is also less than is seen toward the narrow emission lines a nonspherical dust geometry is strongly suggested. The reddening to the broad emission lines should then be the same small value as to the X-ray continuum.

Subject headings: galaxies: individual (NGC 1068) — galaxies: Seyfert — galaxies: X-rays — X-rays: sources — X-rays: spectra

I. INTRODUCTION

No optically selected Seyfert 2 galaxy has been convincingly detected in hard (2–10 keV) X-rays. It has been shown that the narrow-lined ($\sim 10^3$ km s^{-1}) type 2 Seyferts are less X-ray luminous than broad-lined ($\sim 10^4$ km s^{-1}) type 1 Seyfert galaxies (Elvis *et al.* 1978; Kriss, Canizares, and Ricker 1981). This suggests that the two types of Seyfert galaxy are unrelated phenomena. Some authors (Rowan-Robinson 1977; Lawrence and Elvis 1982) have instead proposed that the two types are physically the same except that in type 2 Seyferts the central, broad-line, and continuum emitting regions are obscured from our view by a large amount of dust and gas. This idea stems largely from the discovery of *X-ray selected* narrow-lined AGN. These "X-ray Seyfert 2's" almost all show evidence for strong nuclear reddening. If this idea extends to the optically selected type 2 Seyferts then they should have, at some level, a hard X-ray spectrum similar to that seen in type 1 Seyferts (Mushotzky 1984).

NGC 1068 is the brightest type 2 Seyfert optically and has been widely studied at many wavelengths. The most crucial recent observation is that of Antonucci and Miller (1985) who discovered that the *polarized* optical spectrum of NGC 1068 shows the broad emission line spectrum characteristic of a typical type 1 Seyfert. This suggests that the type 1 nucleus of NGC 1068 is hidden from our view by a "wall" of obscuring material. This wall does not cover the whole sky as seen from the nucleus, and radiation escaping from these other directions can be scattered into our line of sight. Antonucci and Miller specifically propose a model with a thick disk seen edge-on and a warm gas ($T \approx 10^5$ K) above the disk as the scattering medium. This scattered flux produces the polarized optical spectrum observed by Antonucci and Miller. This is an exciting possibility and suggests that all types of Seyfert are indeed the same but for obscuration.

In spite of a tantalizing 4 σ measurement by *Ariel V* (Elvis *et al.* 1978) and a report in the *HEAO* A-1 catalog with a 0.7 deg^2 error box (Wood *et al.* 1984) NGC 1068 has not been convincingly detected as a hard (2–10 keV) X-ray source. It is, however, a strong soft (0.2–3.5 keV X-ray source in *Einstein* IPC observations. Monier and Halpern (1987) find that the IPC spectrum of NGC 1068 is very soft with a power-law energy index (α_E) of ~ 2. This is markedly different from the 2–10 keV spectra seen in type 1 Seyferts and quasars ($\alpha_E \approx$ 0.7–1.0; Mushotzky 1984). The soft X-ray result leaves undecided whether this type 2 Seyfert is really identical to a type 1 but is heavily obscured, or whether some other activity is involved.

In order to search for hard X-ray emission from NGC 1068, we have observed it twice with *EXOSAT*. We have detected hard X-rays from NGC 1068 and have measured their spectrum. We report these findings in this paper and combine them with the *Einstein* data to make a more detailed study of the X-ray spectrum.

II. OBSERVATIONS

NGC 1068 was observed on two separate occasions by *EXOSAT*. Table 1 gives details of the observations. On each occasion the source was detected in the ME (Medium Energy) argon detectors, and in the three energy bands defined by the "thin lexan" (3LX), "aluminum/parylene" (ALP) and boron (BOR) filters in front of the LE CMA (Low Energy Channel Multiplier Array). For details of the *EXOSAT* instrumentation, see Taylor *et al.* (1981). Count rates in each instrument are given in Table 1. The position of the source in the CMA detection is consistent with the optical position (Clements 1981) for the nucleus of NGC 1068.

The counts from the LE filter observations were taken from a square 72″ on a side centered on the X-ray source. This is

TABLE 1

EXOSAT OBSERVATIONS OF NGC 1068

ME[a]		3LX		ALP		BOR	
Exposure	Counts s^{-1}	Exposure	Count Rate[b]	Exposure	Count Rate[b]	Exposure	Count Rate[b]
1983 Day 234:							
34642	0.24 ± 0.02	13750	5.5 ± 0.2	7750	3.1 ± 0.2	9444	0.34 ± 0.06
1985 Day 008:							
41083	0.26 ± 0.02	13305	5.8 ± 0.17	6406	3.1 ± 0.2	4263	0.47 ± 0.09

[a] PHA 6-40.
[b] Per 100 s.

larger than the optical image of the galaxy. The CMA image is dominated by a strong pointlike source out to $\sim 20''$. There is some indication of weak extended emission. This spatial information will be the subject of another paper. The background rate was taken from an identical, source-free, square elsewhere in the field. The obvious background features such as the central stripes were avoided. The count rates were corrected for the fraction of counts outside this region (Davelaar and Giommi 1985) and for the telemetry dead time (Osborne 1985). Corrections for the other effects detailed by Osborne (1985) were included in the spectral fitting procedure and are not included in Table 1.

Background subtraction for the ME was performed according to the method of Smith (1984). The background in each case was taken from the same counters during times when they were pointed away from the source during an "array swap." Periods of high count rate due to solar flares were excluded by visually inspecting the light curves of each detector "half." The data from the "inner" detectors of the ME were much noisier than the "outer" detectors since they are less well shielded against particle background (Arnaud *et al.* 1985). We therefore used only the "outer" detectors in our analysis. Figure 1 shows the resultant PHA (pulse height analysis) distributions for each observation. The source is detected over the PHA range 6–40 which corresponds to 2–10 keV.

The ME count rate corresponds to 0.6 μJy at 2 keV or 6.1×10^{-12} ergs cm^{-2} s^{-1} (2–10 keV). This implies a 2–10 keV luminosity of 3.6×10^{41} ergs s^{-1} for a distance of 22 Mpc to NGC 1068 (based on its redshift of 1109 km s^{-1} (de Vaucouleurs, de Vaucouleurs, and Corwin 1976) and a Hubble constant $H_0 = 50$ km s^{-1} Mpc^{-1}). This is consistent with the 3 σ upper limit of $<5 \times 10^{41}$ ergs s^{-1} (2–10 keV) reported by Monier and Halpern (1987) from the Monitor Proportional Counter on the *Einstein Observatory*.

The field of view of the ME is large (FWHM = 45′) so we may expect some hard X-ray emission from normal X-ray sources distributed throughout the galaxy. A normal Sb spiral galaxy similar to NGC 1068 ($T = 3$; de Vaucouleurs, de Vaucouleurs, and Corwin 1976) of the same absolute optical magnitude has a luminosity in the range $1\text{–}10 \times 10^{39}$ ergs s^{-1} (0.2–3.5 keV; Fabbiano and Trinchieri 1985) and has a hard spectrum with no intrinsic low energy cutoff (Fabbiano and Trinchieri 1987) so that its 2–10 keV luminosity is similar. The narrow distribution of X-ray to optical flux density for early-type spirals (Fabbiano and Trinchieri 1985) allows us to predict the X-ray flux of NGC 1068 to within a factor of about 3. The mean X-ray to optical ratio predicts an X-ray flux of 0.1 μJy (using $B_T{}^0 = 9.17$ from de Vaucouleurs, de Vaucouleurs, and Corwin 1976). This is a factor of 6 below the observed ME value. The largest X-ray to optical ratio seen in normal early-type spirals would give an X-ray flux of 0.4 μJy, which could dominate the ME flux density. On this basis alone then we cannot unambiguously decide whether or not the ME detection is due to nuclear emission. The comparison of the IPC and CMA count rates made in the next section, however, indicates that very little of the 1 keV flux comes from outside the central 20″ diameter region. The amount of distributed emission from the body of the galaxy is therefore small compared with the ME count rate. We conclude that it is safe to assume that the bulk of the ME flux density originates in the nuclear region of NGC 1068.

There is no evidence for broad-band variability between the two *EXOSAT* observations (see Table 1). Neither is there any evidence within the ME observations for variability of amplitude greater than $\sim 20\%$ on time scales down to ~ 30 minutes. There are too few counts to give useful variability limits within the individual LE filter observations.

The *Einstein* IPC (Imaging Proportional Counter; Giacconi *et al.* 1979, Gorenstein, Harnden, and Fabricant 1981) observations have been reported by Monier and Halpern (1987). There were three IPC observations, all in 1979 (January 19, July 22, August 1). Each of them was short (~ 20 minutes). We have used the same observations here in a joint spectral fit.

III. SPECTRAL FITS

a) *EXOSAT Data: Spectral Curvature*

We first fitted a simple power-law plus absorption model[1] to each of the two *EXOSAT* ME observations. Fits a and b in Table 2 gives the results. The errors on each fit are large, but the error regions overlap greatly in all three parameters, including normalization. There is thus no evidence for variability between the two *EXOSAT* ME observations, and so they can reasonably be combined.

The results of a joint fit to these two data sets is given in fit c of Table 2 and contours of allowed (N_H, α_E) combinations for the combined ME data set are shown in Figure 2. The constraints on α_E are much better defined in this joint fit and clearly exclude the values obtained by Monier and Halpern (1987) for their lower energy IPC fit (see also our fit f in Table 2 and Fig. 2). This strongly suggests that the source spectrum has curvature, flattening to higher energies (or steepening to low energies, depending on your perspective). Spectral variability of the source between the 1979 IPC observations and the 1983 ME observations could however give the same effect.

[1] $f_\nu \propto \nu^{-\alpha_E} e^{-N_H \sigma}$; cross sections were taken from Morrison and McCammon (1983).

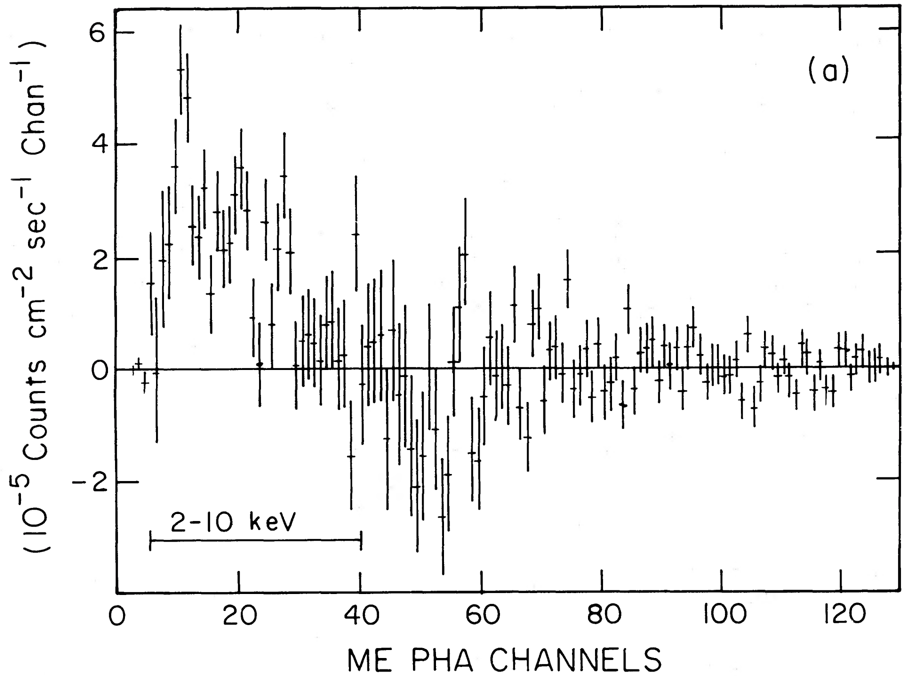

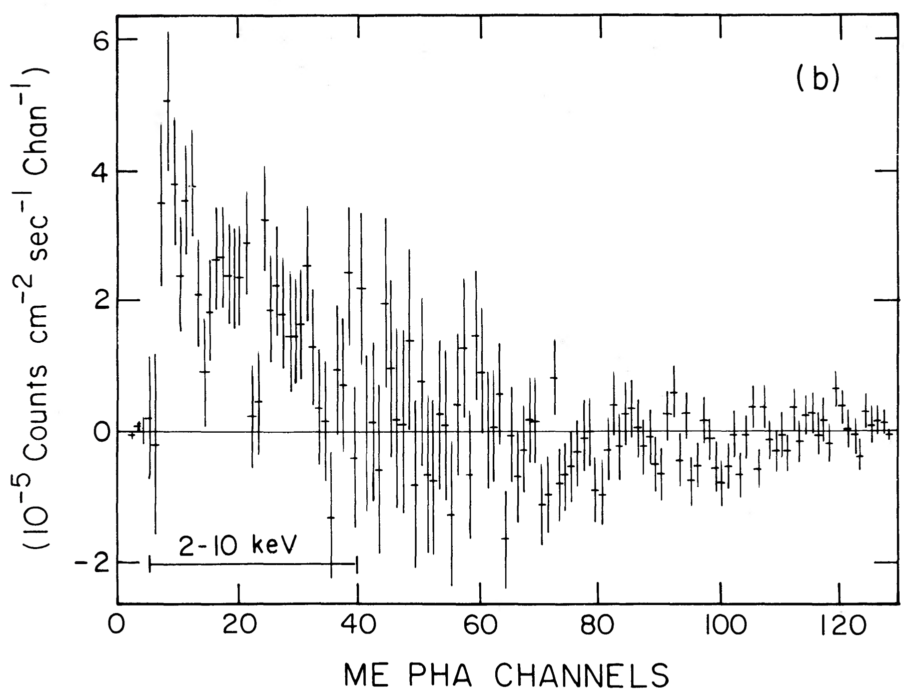

FIG. 1.—Background-subtracted *EXOSAT* ME PHA distributions for the (*a*) 1983 day 234, (*b*) 1985 day 8 observations of NGC 1068. Only the "outer" detectors were used. The channels corresponding approximately to the 2–10 keV range are marked.

The existence of this spectral curvature is reinforced by the addition of the simultaneous LE data. A joint fit to the ME and LE data gives an acceptable χ^2 (fit d, Table 2), but only if the column density is $< 1.5 \times 10^{18}$, far below the Galactic value $(3.05 \pm 0.1) \times 10^{20}$ atoms cm^{-2} (Elvis and Lockman 1988). If the column density is constrained to be at least the Galactic value then the fit becomes unacceptable with a probability of being produced of 0.002 (fit e in Table 2). A more complex spectrum is certainly required.

The *EXOSAT* data establish two major new points: (1) There is hard (2–10 keV) X-ray emission from NGC 1068; and (2) this hard emission has an energy spectral slope of ~ 0.7 similar to that of type 1 Seyfert galaxies (in the same energy range). The lack of low energy absorption, although apparently a more stringent limit that than that of Monier and Halpern, is ambiguous because of the complex low-energy spectrum. A combination of *EXOSAT* and IPC data can help to unravel this complexity.

TABLE 2

ONE-COMPONENT POWER-LAW FITS TO *EXOSAT* AND *Einstein* DATA FOR NGC 1068

Fit	Data Fitted	α_E[a]	N_H[a,b]	χ^2	d.o.f.[c]	Normalization[d]
a.........	ME, 83/234	0.45 ± 0.65	<109	171	137	$0.67^{+0.99}_{-0.40}$
b.........	ME, 85/008	$0.68^{+0.77}_{-0.47}$	<163	205	207	$0.98^{+2.07}_{-0.46}$
c.........	ME, both dates	$0.68^{+0.34}_{-0.47}$	<70	378	347	$0.94^{+0.58}_{-0.44}$
d.........	ME + LE, both dates	0.67 ± 0.08	<0.0033	381	350	$0.93^{+0.11}_{-0.09}$
e.........	d with $N_H \geq N_H$(Gal)	1.60 ± 0.15	$2.95^{+0.68}_{-0.0}$	417	350	0.26 ± 0.04
f.........	IPC[e], all data	$2.05^{+0.51}_{-0.43}$	$5.25^{+2.6}_{-2.0}$	22	19	$2.80^{+2.40}_{-0.64}$
g.........	All data	1.48 ± 0.20	2.63 ± 1.0	450	372	$2.31^{+0.34}_{-0.32}$

[a] 90% confidence ranges for three interesting parameters (χ^2_{min} + 6.25; Avni 1976).
[b] 10^{20} atoms cm^{-2}.
[c] Degrees of freedom.
[d] μJy at 1 keV.
[e] PHA 2-12.

b) *Consistency of EXOSAT and Einstein Data*

The changing spectral slope makes it difficult to compare the IPC and *EXOSAT* data. We can make one comparison at 1 keV since this is roughly the effective energy of the IPC for most spectra (Harnden *et al.* 1984). This is similar to that of the BOR filter of the LE. We have used the best fit to the combined IPC observations (Table 2) to predict the BOR count rate. This gives a BOR count rate of 7.45×10^{-5} counts cm^{-2} s^{-1} compared with the observed rates of $(7.66 \pm 1.47) \times 10^{-5}$ counts cm^{-2} s^{-1} and $(5.52 \pm 0.98) \times 10^{-5}$ counts cm^{-2} s^{-1}, deviations of 0.0 and 2.0 σ, respectively. A second comparison can be made at 2 keV since here the ME and IPC both have significant response. The joint ME fit (fit c, Table 2) has a photon count rate of 4.9×10^{-4} photons cm^{-2} s^{-1} keV^{-1} at 2 keV. By comparison the joint IPC fit (fit f, Table 2) has 4.4×10^{-4} photons cm^{-2} s^{-1} keV^{-1} at 2 keV, which is consistent within the errors with the ME. The IPC data thus show no sign of variability compared with the *EXOSAT* data.

Since we already know that there is no evidence of variability within the IPC or the *EXOSAT* data, the entire data set can thus be reasonably combined in a joint fit. The lack of variability in this source over a 4 yr period is itself noteworthy and will be discussed later.

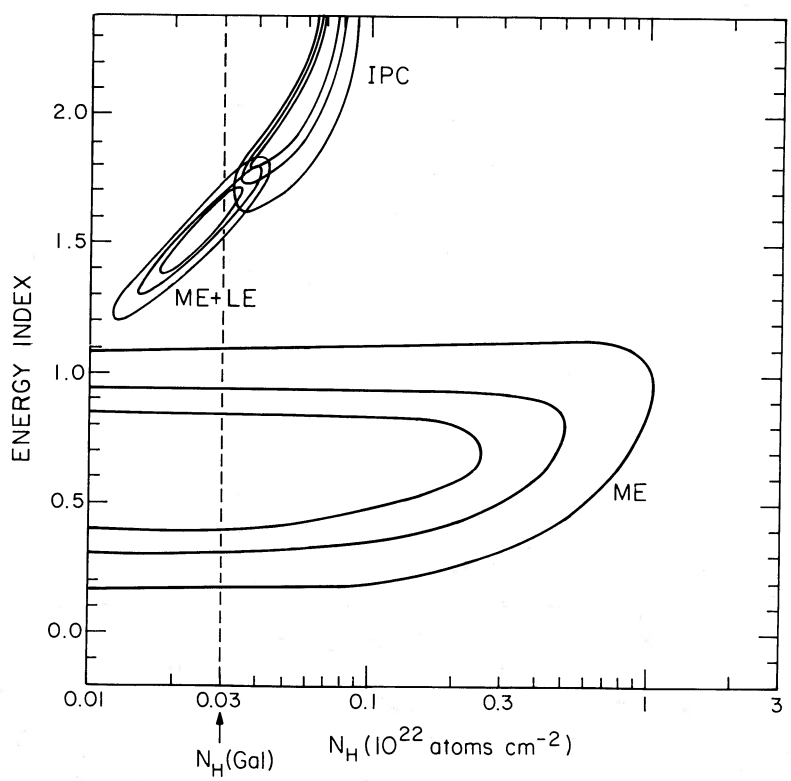

FIG. 2.—Allowed ranges of energy spectral index, α_E, and absorbing column density, N_H, for a single power-law fit to the combined *EXOSAT* ME data (ME), the combined *EXOSAT* ME and LE data (ME plus LE), and the IPC data (IPC) for NGC 1068. Contours at 68%, 90%, and 99% confidence for two interesting parameters are shown in each case. The Galactic column density is shown with the vertical dashed line.

A fit to all the *EXOSAT* and *Einstein* data gives an unacceptable χ^2 ($P_{random} = 0.003$) although it finds a range of N_H that is extremely close to the Galactic hydrogen column density. This is a reflection of the spectral curvature noted in the previous section. Clearly a more complicated model is needed to describe the data.

c) *Two-Component Fits*

The next simplest fit beyond a single power-law plus absorption fit is a two power-law fit, where both power laws suffer the same absorption. We have fitted two power laws and a column density. The resulting allowed range of the two power-law indices are plotted in Figure 3*a* and the values given in Table 3.

Both power-law ranges are large. The first component tends to very flat values (<0.0) but does include most of the range seen at higher energies in Seyfert 1 galaxies (Mushotzky 1984). A slope of 1.0, such as is found for radio-quiet quasars in the IPC energy range (Wilkes and Elvis 1987) is excluded at the $\sim 90\%$ level. The second component prefers values similar to

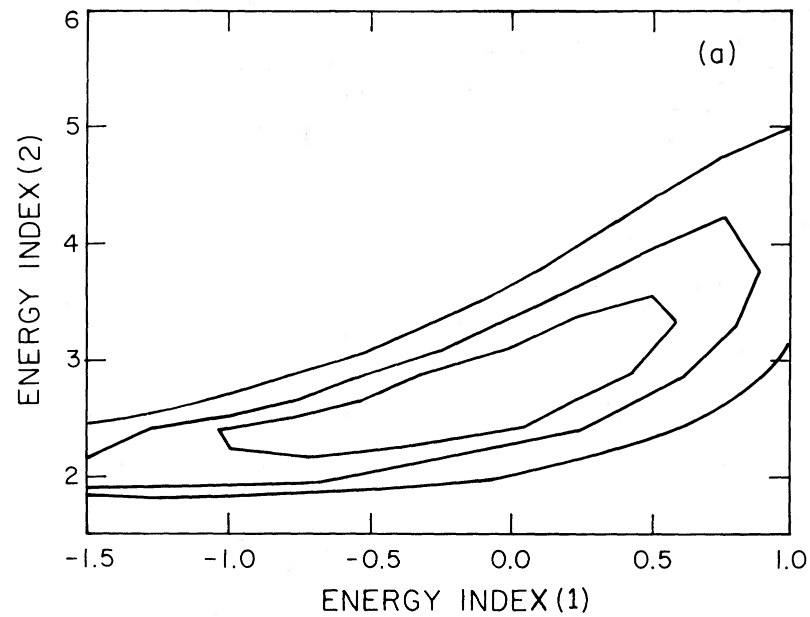

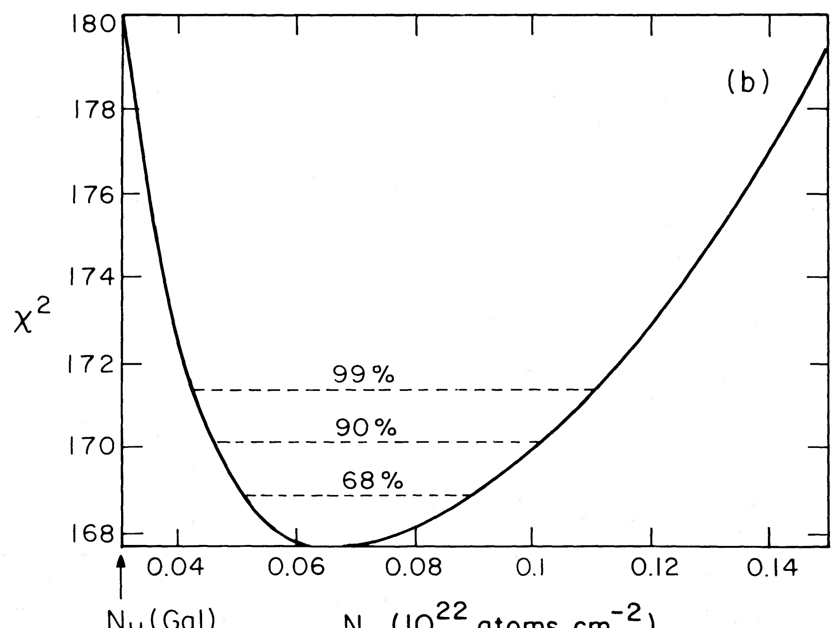

FIG. 3.—Results of a two-component power-law fit to all of the *EXOSAT* and *Einstein* data for NGC 1068. A single hydrogen absorption column was applied to both components. (*a*) Allowed ranges of the two power-law energy indices. Contours at 68%, 90%, and 99% confidence for two interesting parameters are shown in each case. (*b*) Allowed range of N_H (the Galactic column density is shown at the left axis). χ^2 levels corresponding to 68%, 90%, and 99% confidence intervals for one parameter are shown.

TABLE 3

TWO-COMPONENT FITS TO ALL DATA FOR NGC 1068

$\alpha_E(1)$[a]	kT (keV) or $\alpha_E(2)$[a]	N_H[a,b]	χ^2[c]	Norm(1)[a,d]	Norm(2)[a,d]
		Two Power-Law Fit			
$-0.69^{+0.13}_{-0.10}$	$2.29^{+1.05}_{-0.53}$	$6.3^{+3.9}_{-2.3}$	392	$0.086^{+0.046}_{-0.074}$	$2.72^{+0.46}_{-0.56}$
$-1.88^{+0.23}_{-0.15}$	$1.64^{-0.11}_{-0.08}$	$\equiv N_H$(Gal)	409	$0.006^{+0.045}_{-0.006}$	$2.3^{+0.16}_{-0.18}$
		Power-Law plus Bremsstrahlung Fit			
-0.08 ± 0.10	0.54 ± 0.2	$2.5^{+0.9}_{-1.5}$	397	$2.93^{+0.37}_{-0.09}$	$1.35^{+0.07}_{-0.09}$
$-0.13^{+0.69}_{-0.56}$	$0.55^{+0.0}_{-0.16}$	$\equiv N_H$(Gal)	398	$0.27^{+0.48}_{-0.21}$	$13.9^{+3.3}_{-2.3}$
		Power-Law plus Optically Thermal Plasma Fit[e]			
0.85 ± 0.10	$0.19^{+136}_{-0.08}$	$3.0^{+5.7}_{-1.3}$	416	$1.2^{+0.6\,f}_{-0.1}$	$2.62^{+11.1\,f}_{-0.23}$
0.85 ± 0.32	0.19 ± 0.03	$\equiv N_H$(Gal)	416	$1.19^{+0.48\,f}_{-0.37}$	$2.64^{+0.53\,f}_{-0.80}$
		Power-Law plus Blackbody Fit			
$0.38^{+0.19}_{-0.08}$	0.20 ± 0.02	$0.0^{+0.08}_{-0.0}$	395	0.60 ± 0.06	0.07 ± 0.01
$0.43^{+0.08}_{-0.11}$	0.43 ± 0.02	$\equiv N_H$(Gal)	402	$0.62^{+0.08}_{-0.06}$	0.19 ± 0.01

[a] Uncertainties are $\chi^2_{min} + 6.25$.
[b] The same absorbing N_H is applied to each component and is free, or is equal to N_H(Galactic) where noted by $\equiv N_H$(Gal), i.e., $= 3.0 \times 10^{20}$ atoms cm^{-2}.
[c] Note: degrees of freedom $= 370$ for N_H free; $= 372$ for $N_H = N_H$(Gal).
[d] μJy at 1 keV.
[e] Raymond and Smith 1977, Raymond 1980, private communication, using cosmic abundances.
[f] Emission measure, $\int n_e n_p \, dV$ (10^{64} cm^{-3}), for a distance of 22 Mpc.

the extremely steep slope value found for the quasar PG 1211+143 by Bechtold *et al.* (1987) and the low-luminosity Seyfert 1 nucleus of M81 (Fabbiano 1987).

The allowed values of absorption in the two power-law model are shown in Figure 3*b*. The Galactic value (3.05×10^{20} atoms cm^{-2}) is clearly excluded in this model. The implied value of additional absorption, which would presumably be intrinsic to the source, is similar to the Galactic value and could, for example, be due to the interstellar medium in the outer regions of NGC 1068. We caution, however, that the N_H value derived is heavily dependent on the continuum form assumed before absorption.

An alternative continuum form to replace the steep low-energy power law would be a thermal model—bremsstrahlung, an optically thin plasma (Raymond and Smith 1977; Raymond 1980), or a blackbody. Such a form may have physical significance in terms of, e.g., a hot confining medium for the emission line regions (Krolik, McKee, and Tarter 1981); hot gas ejected from the nucleus as in M82 or NGC 253 (Watson, Stanger, and Griffiths 1984; Fabbiano and Trinchieri 1984); or the hottest part of an accretion disk spectrum (Czerny and Elvis 1987). All three forms give acceptable fits. Details are given in Table 3. The low-energy curvature of these forms allows the Galactic N_H to give a good fit and hence no requirement for any intrinsic absorption in NGC 1068.

As an example of these fits we give the allowed temperatures and power-law indices in Figure 4*a* and the allowed N_H values in Figure 4*b* for the blackbody plus power-law case. In neither the power law nor any of the thermal cases (Table 3; Figs. 3, 4) is an N_H greater than 10^{21} atoms cm^{-2} allowed.

d) Fe-*Line Limits*

Strong fluorescent iron line emission with an equivalent width over 1 keV is expected if all the X-rays from NGC 1068 are electron scattered via a warm gas (see § III*d*, below; Antonucci and Miller 1985; Makishima 1986; Krolik and Begelman 1987; Krolik and Kallman 1987). We have therefore fitted the ME data with a power-law plus line model.

First we fitted a power law with absorption to the ME data excluding the 6–8 keV region in which the Fe K line would appear. We then froze the power-law parameters and made a fit of a Gaussian line of width 0.1 keV and variable line center to just the 6–8 keV region.

There is evidence for the detection of an iron line in the data. We find a best-fit equivalent width of $2.6^{+0.6}_{-0.8}$ (68% confidence) keV. Figure 5 shows the χ^2 versus the line equivalent width. A 99% upper limit to the line equivalent width is 4.8 keV and a similar lower limit is 0.62 keV. The values we find are large and similar to those predicted within a scattering model. These ranges only take into account statistical errors, however. At low count rates such as for NGC 1068, systematic errors dominate. These can be judged from the best fit of an iron line to the data as shown in Figure 6. Other regions of the ME spectrum where no line is expected show almost as large deviations from the power-law model so that our line detection must be tentative and cannot be considered alone as decisive evidence in favor of scattering.

IV. DISCUSSION

The detection of hard X-ray emission with a spectrum typical of type 1 Seyfert galaxies was posed by Monier and Halpern (1987) as the best test for the Antonucci and Miller (1985) hypothesis that NGC 1068 is a normal type 1 Seyfert galaxy hidden behind a "wall" of dust and gas and seen by us only in reflection. We have now detected such X-ray emission from NGC 1068 and have determined the power-law slope over the 2–10 keV range ($\alpha_E = 0.68 \pm 0.25$; fit c, Table 2) to be the same as that of type 1 Seyferts (in the same energy range). Thus not only are the emission line properties of the hidden nucleus indistinguishable from a normal Seyfert 1 but so are the observable continuum properties. It is now hard to doubt that there is a normal type 1 Seyfert nucleus in NGC 1068. The

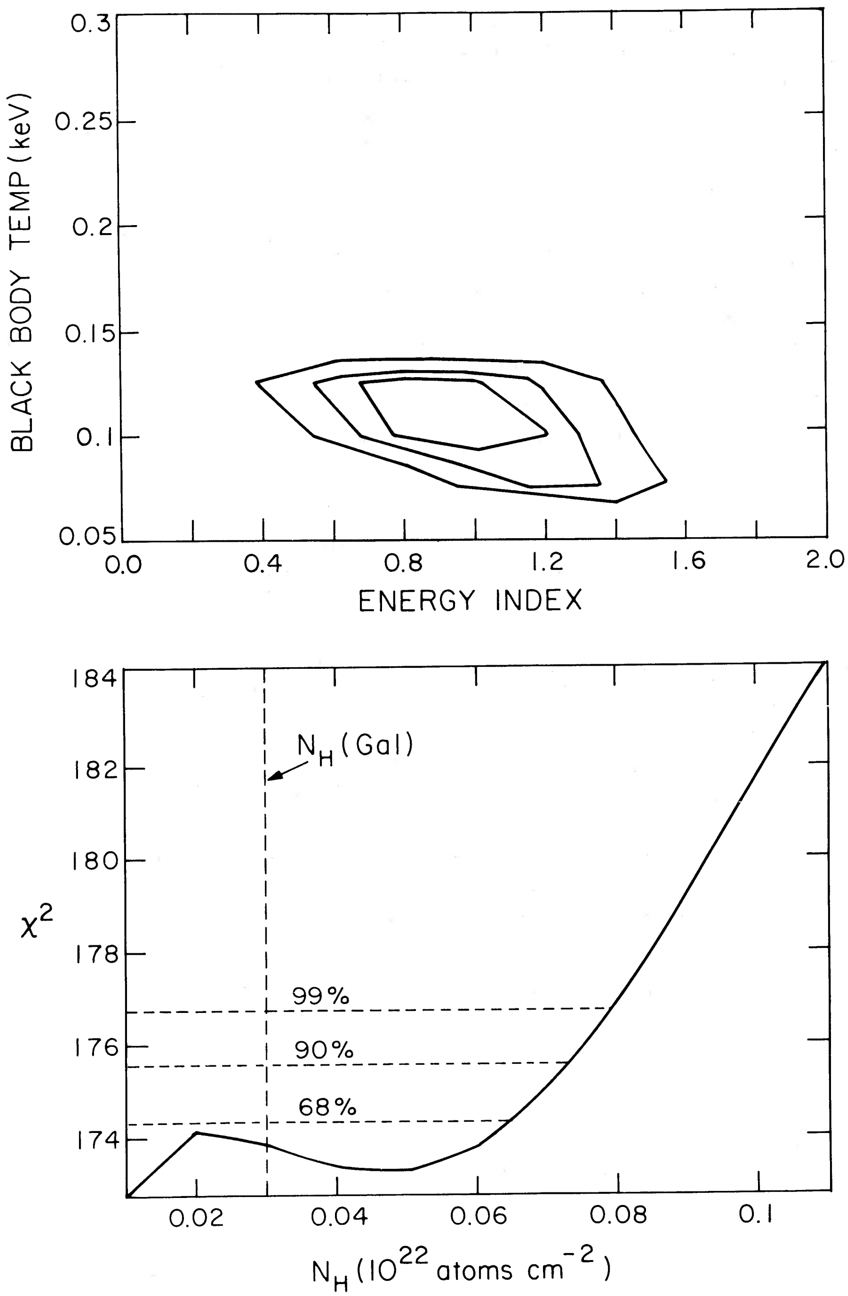

FIG. 4.—Results of a two-component power-law plus blackbody fit to all of the *EXOSAT* and *Einstein* data for NGC 1068. A single hydrogen absorption column was applied to both components. (*top*) Allowed ranges of the power-law energy index and blackbody temperature. Contours at 68%, 90%, and 99% confidence for two interesting parameters are shown in each case. (*bottom*) Allowed range of N_H. The Galactic column density is shown with the vertical dashed line. χ^2 levels corresponding to 68%, 90%, and 99% confidence intervals for one parameter are shown.

question remains of whether we see it in X-rays directly or in scattered light since it is possible to completely block Hβ but allow through hard X-rays. The X-ray data allow us to deduce more about the system.

a) *Lack of Absorption*

No intrinsic column density greater than 10^{21} atoms cm^{-2} is seen in the X-ray spectrum of NGC 1068 even in two-component fits. This argues that the X-rays are not coming to us *through* an obscuring region, although the soft X-rays could mask an absorption in the hard X-rays if they come from outside the absorbing cloud.

Snijders, Netzer, and Boksenberg (1986) have suggested that the ultraviolet emission from NGC 1068 is scattered not by electrons but by dust. The choice between the two scatterers has depended on the intricate problem of the subtraction of galaxy starlight to give the wavelength dependence of the polarization of the nuclear spectrum. The X-ray spectrum gives a much more direct test. Dust scattering would lead to a strong low energy absorption of X-rays since dust would have a large

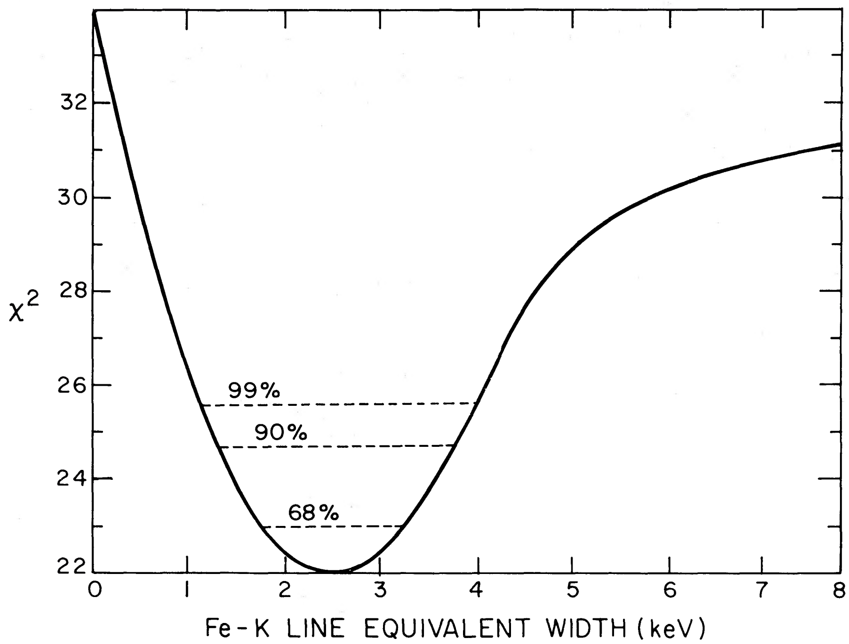

FIG. 5.—Allowed range of iron-line equivalent width between 6 and 8 keV. A single power law was first fitted to the combined *EXOSAT* ME data after excluding the 6–8 keV region. χ^2 levels corresponding to 68%, 90%, and 99% confidence intervals for one parameter are shown.

absorption cross section up to several keV. The lack of low-energy absorption in NGC 1068 implies that the X-rays are not coming to us after being scattered off a dust cloud. The scattering mechanism in NGC 1068 is thus electron scattering. Monier and Halpern have stressed that an electron scattering gas must be photoionized up to the point at which (at least) oxygen is fully stripped in order for it to not absorb the soft X-rays. (A thermally ionized gas would need to be at $\sim 10^7$ K, which is disallowed by the observed line widths.) The scatterer is thus probably fairly close to the nuclear ionizing source.

Neugebauer *et al.* (1980) find that the narrow optical emission lines in NGC 1068 indicate a reddening of $E(B-V) = 0.4$. This corresponds to $N_H = 3 \times 10^{21}$ atoms cm^{-2} for standard interstellar conditions (Jenkins and Savage 1974). This is inconsistent with both the one- and two-component fits to the joint X-ray data. While it is possible that other continuum

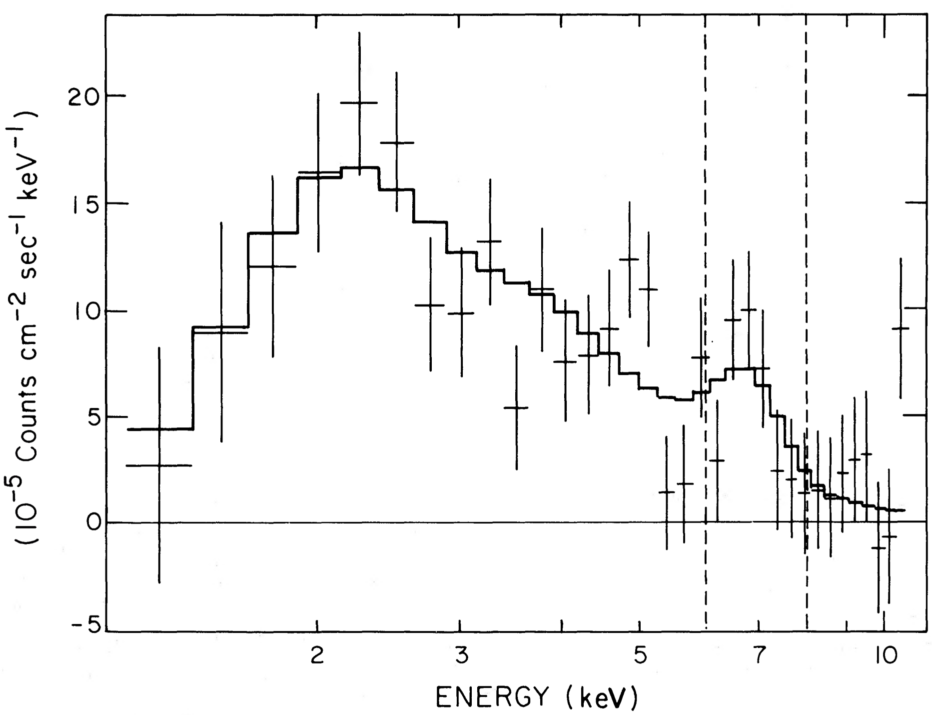

FIG. 6.—The best-fit power-law plus single line spectrum folded through the *EXOSAT* ME response compared with the combined ME PHA data, channels 6–40. The 6–8 keV range, which was left out of the power-law fit, is marked with vertical dashed lines.

models might allow this high absorption, it is more plausible that the X-ray continuum, like the UV (Snijders, Netzer, and Boksenberg 1986), does not possess absorption features. This could have two causes: either the X-ray and UV continuum comes to us via a cleaner line of sight than the emission lines or the absorbing medium has a higher dust-to-gas ratio than the local Galactic interstellar medium.

Depleted dust-to-gas ratios are easy to understand near a strong continuum source since evaporation and scattering are likely to destroy dust grains. Maccacaro, Perola, and Elvis (1982) and Mushotzky (1982) invoke low dust-to-gas ratios to reconcile large X-ray column densities with lower optical reddening in several X-ray selected Seyfert 1.9 and 2 galaxies. *Enhanced* dust-to-gas ratios are, however, not readily produced.

The narrow line emitting gas must be further from the central continuum source than the scattering gas else it too would be photoionized (given its small optical depth). An unusual geometry for the reddening-producing material is needed to allow a clear line-of-sight closer to the nucleus than further out. A spherical distribution will affect the continuum as much, or more, than the forbidden lines. A conical geometry, suggested by the obscuring torus model, can give the right effect if it is shared by the reddening material. This requires that the dust exist only in this cone, and then only beyond the radius at which the continuum scattering occurs. If the scattering material is an outflowing wind (Krolik and Begelman 1987) the cooling of this wind from the scatterer temperature of $\sim 10^5$ K to a few 100 K further out would allow the formation of dust. A prediction of this geometry is that the scattered broad lines should be reddened only to the same extent as the continuum.

The column density of obscuring material needed to block direct 2–10 keV X-rays is $\sim 10^{25}$ atoms cm^{-2} (Kallman and Mushotzky 1985). At these energies Compton scattering becomes important. Kallman and Mushotzky show that the combination of the effect of Compton scattering in softening the spectrum and in increasing the path length for a photon to escape the medium leads to increased photoabsorption. Even the hard X-ray spectrum is thus suppressed at these column densities. There is further evidence for an extremely large column density toward the nucleus of NGC 1068. A strong water maser is seen in NGC 1068 (Claussen, Heiligman, and Lo 1984) at 1.35 cm. This maser is small in angular size (<35 mas) and highly variable (by a factor 2 in 8 months) (Claussen and Lo 1986).

Heavy obscuration reopens the possibility of radiative pumping for this H_2O maser. Claussen and Lo point out that the observed luminosity of NGC 1068 at 6 μm is barely sufficient to provide radiative pumping for the H_2O maser if the maximum possible efficiency is assumed. They conclude that some other pumping mechanism is probably at work. This argument assumes that the observed 6 μm luminosity of NGC 1068 is the luminosity seen by the maser. The obscuration model for NGC 1068 weakens this argument substantially. Reddening in the mid-infrared is normally an insignificant consideration, but here this may not be the case. Although Galactic reddening at 6 μm is poorly determined its value is of order $\sim$3%–6% of that in the visual (A_V) (see, e.g., Willner 1984). The column densities needed to suppress the direct hard X-ray emission, however, correspond to $A_V \approx$ 3000! This gives $\sim$100–200 mag of extinction at 6 μm. In support of this is DePoy's (1987) finding that the absence of broad Brackett lines in NGC 1068 implies $A_V \gtrsim 100$. The X-ray column density may overestimate the dust extinction since close to the X-ray source dust should be evaporated. In active galaxies for which both X-ray and optical extinction can be estimated, the X-ray column density is typically larger by a factor ~ 10 (Maccacaro, Perola, and Elvis 1982). Nevertheless the two extinctions correlate and even 10–20 mag of extinction at 6 μm is large. With so much extinction applied the observed 6 μm flux density would be only the scattered fraction. The scattered fraction is unknown, although Antonucci and Miller argue that it may be of the order 10%. The 6 μm luminosity available to radiatively pump the H_2O maser could thus easily exceed the observed value by a large factor and so remove the radiative pumping efficiency problem.

b) *Hard X-Ray Spectrum*

The suggestive results on the presence of an iron emission line at 6.4 keV are an indication in favor of the scattering model. Scattering models predict an equivalent width for the Fe Kα line that depends primarily on the fluorescent yield of iron. Makishima (1986) predicts equivalent widths >2 keV for this feature in a similar geometry for Galactic X-ray sources. Krolik and Kallman (1987) predict similar equivalent width for NGC 1068, depending on the ionization state. These are consistent with our measurements. However, the quality of the ME spectrum is insufficient to be certain of this feature.

The 2–10 keV spectrum gives a best fit slope of ~ 0.7 and its similarity to the measured index in type 1 Seyfert galaxies in the same energy range supports the obscuration model. It is not necessarily the case though that this slope has physical significance. Wilkes and Elvis (1987) have argued that the $\alpha_E \approx$ 0.7 index in type 1 Seyferts is the result of the mixing of two other components with slopes of ~ 0.4 and ~ 1.0. It is notable that the (required) two-component fits of § III*b* (Table 3) do not prefer a 0.7 index. Only higher quality X-ray spectra extending to higher energies can decide this issue.

Since the brightest type 2 Seyfert galaxy is a hard X-ray source with a flat spectrum similar to a type 1 Seyfert the possibility occurs that all Seyfert 2 galaxies behave similarly and so might contribute significantly to the X-ray background. In IRAS selected lists type 2 Seyferts are several times more common than type 1 Seyferts (Leech *et al.* 1987; Lawrence 1987) and there is also the possibility that high IR luminosity galaxies in general, which have a very large space density (Lawrence *et al.* 1986; Soifer *et al.* 1986), may also be obscured Seyferts (e.g., De Poy, Becklin, and Wynn-Williams 1986; Norris 1985). The "obscured AGN" contribution to the X-ray background may then be quite large. A proper study of this question is under way using the *IRAS* luminosity functions.

c) *Steep Soft X-Ray Component*

The complex X-ray spectrum of NGC 1068 is similar to that of several active galaxies with broad emission lines. Many quasars are now known to have ultrasoft excesses (Elvis, Wilkes, and Tananbaum 1985; Arnaud *et al.* 1985; Pounds *et al.* 1987; Wilkes and Elvis 1987). Recently the low-luminosity nucleus of M81 (Fabbiano 1987) has been found to have a steep low-energy spectrum so that this phenomenon is not confined to high luminosity objects.

These excesses are usually modeled in terms of thermal accretion disk emission. We can do the same for NGC 1068. A major constraint in these models is the total luminosity in the continuum in the optical/ultraviolet region. The slope of the short wavelength ultraviolet continuum is -1.2 ± 0.3 (Monier and Halpern 1987). This is in the range given by simple thin accretion disk models (e.g., Shakura and Sunyaev 1973). In NGC 1068 the ultraviolet luminosity is uncertain both because of normal reddening (Snijders, Netzer, and Boksenberg 1986) and by an unknown factor because we do not know the fraction of the continuum that is scattered toward us. For the *observed* ultraviolet continuum luminosity at 1311 Å of 3.31×10^{-26} ergs cm^{-2} s^{-1} Hz^{-1} (Monier and Halpern 1987) assuming a peak in the νf_ν distribution at $10^{16.38}$ Hz ($\equiv$0.1 keV) in order to give the soft X-ray spectrum (as in PG 1211+143; Bechtold *et al.* 1987) then the relations given by Bechtold *et al.* (1987) yield a central mass of $10^{5.6}$ $M_\odot$ and an accretion rate of $10^{-1.7}$ $M_\odot$ yr^{-1}. If we are instead seeing only 0.1 of the total continuum luminosity then these values become $10^{6.1}$ $M_\odot$ and $10^{-0.7}$ $M_\odot$ yr^{-1}. These accretion rates are sub-Eddington so the simple thin disk approximation used to derive them is self-consistent, a situation that does not hold for the more luminous quasars (Czerny and Elvis 1987).

We find it surprising that the values of the accretion rate in active galaxies should scale with the central mass so as to give very much the same soft X-ray spectrum over a range of 10^{2-3} (cf. Czerny and Elvis 1987; Fabbiano 1988). It is possible, however, there may be some selection effect at work. For instance, only those active galaxies that show steep soft X-ray spectra have the accretion disk models applied to them. They may thus be the extreme cases of a distribution. On the other hand, disk models may be inappropriate and some other mechanism is in fact at work. The thermal models fitted in the previous section indicate some possibilities.

d) Absence of Variability

We see no variability on timescales from 30 minutes to 4 yr. Rapid X-ray variability is seen in other AGN (e.g., NGC 4051; Lawrence *et al.* 1987) and there is some indication that it is more common in nuclei of lower luminosity (Tennant and Mushotzky 1983). M81, which is similar to NGC 1068 in both its observed nuclear X-ray luminosity and its X-ray spectrum, has been seen to vary by a factor of 2 in only 10 minutes in soft X-rays (Barr, Mushotzky, and Giommi 1988). No such behavior is seen in NGC 1068. A similarly unusual lack of variability was noted by Snijders, Netzer, and Boksenberg (1986) in the ultraviolet. In any scattering model variations would be smeared out if on a time scale shorter than $\Delta t = (\tau + 1)R/c$, where τ is the scattering optical depth, R is the size of the scattering region, and c is the speed of light. The observed lack of variability is then so far consistent with models involving a scattering region of size $\sim$1 pc and modest opacity (e.g., Krolik and Begelman 1986).

Lack of variability would also be expected if the X-rays originated in an extended region. Since thermal models of the steep soft component are acceptable, this possibility cannot be ruled out.

The lack of X-ray variability in NGC 1068 is especially remarkable since, as described above, the nucleus contains a highly variable H_2O maser (Claussen and Lo 1986). They report a reduction by a factor of 2 in the 1.35 cm H_2O maser line strength in the 8 months from 1983 September to 1984 May, i.e., between the two *EXOSAT* observations. Claussen and Lo suggest that the maser is saturated, and so the variations do not reflect changes in the pumping continuum source. However, we pointed out above that radiative pumping could in fact produce the maser emission if the true 6 μm luminosity is much greater that the observed value due to extinction. In this case the variations in the 1.35 cm line may reflect underlying changes in the nuclear continuum. The lack of observed changes in the X-ray band would then strongly suggest that some smoothing of the X-ray light curve has taken place via a scattering region.

V. CONCLUSIONS

NGC 1068 has a hard (2–10 keV) spectrum similar to those of type 1 Seyferts. This strongly suggests, given the presence of broad emission lines in the polarized optical spectrum of the galaxy, that NGC 1068 is a normal type 1 Seyfert galaxy in which we do not see the nucleus directly but only in reflection. Since there is no soft X-ray absorption, the scattering must be from a photoionized electron scattering region, rather than dust. The lack of X-ray absorption also requires a nonspherical geometry for the dust that reddens the narrow-line region. A conical geometry, with dust forming only beyond the radius of the scattering region, would fit the observations.

Several other X-ray observations in this paper support the scattering picture: The lack of variability is unusual, especially in the context of the highly variable H_2O maser, but it is easily understood if the scattering region has an extent of $\sim$1 pc; the steep soft X-ray spectrum is similar to that seen in a number of type 1 Seyferts and quasars; and there is marginal evidence for the presence of a strong (EW $\approx$ 2.5 keV) iron line. Such a line is expected in the scattering model from fluorescence.

More exacting tests of this model are possible. A high-quality, high-resolution X-ray spectrum around the iron line energy could rule out the model if no line is found. If a line were seen, then measurement of the line energy would determine the ionization parameter of the scattering gas. X-ray polarization should be another strong diagnostic since, in this model, all the hard X-rays that we see are scattered and so should be highly polarized ($\sim$20%) like the broad lines. A sensitive X-ray telescope could extend these studies to the general population of type 2 Seyferts and so fit them into the broader context of galaxy activity.

We thank K. Arnaud, R. Shafer, and A. Tennant for their work on the XANADU data analysis system. XANADU was originally implemented at the Institute of Astronomy, Cambridge. We also thank J. Lockman for advice on the Galactic hydrogen structure. The IPC data came from the *Einstein* data bank. This work was supported in part by NASA grant NAG8-568 and by NASA contract NAS8-30751.

REFERENCES

Antonucci, R. R., and Miller, J. S. 1985, *Ap. J.*, **297**, 621.
Arnaud, K. A., *et al.* 1985, *M.N.R.A.S.*, **217**, 105.
Avni, Y. 1976, *Ap. J.*, **210**, 642.
Barr, P., Mushotzky, R. F., and Giommi, P. 1988, *Ap. J.*, submitted.
Bechtold, J., Czerny, B., Elvis, M., Fabbiano, G., and Green, R. F. 1987, *Ap. J.*, **314**, 699.
Claussen, M. J., Heiligman, G. M., and Lo, K.-Y. 1984, *Nature*, **310**, 298.
Claussen, M. J., and Lo, K.-Y. 1986, *Ap. J.*, **308**, 592.
Clements, E. D. 1981, *M.N.R.A.S.*, **197**, 829.
Czerny, B., and Elvis, M. 1987, *Ap. J.*, **321**, 305.
Davelaar, J., and Giommi, P. 1985, *EXOSAT Express*, No. 10, p. 45.
DePoy, D. L. 1987, in *Infrared Astronomy with Arrays*, ed. C. G. Wynn-Williams and E. E. Becklin (Honolulu: University of Hawaii Press), p. 426.
DePoy, D. L., Becklin, E. E., and Wynn-Williams, C. G. 1986, *Ap. J.*, **307**, 116.
de Vaucouleurs, G., de Vaucouleurs, A., and Corwin, H. G. 1976, *Second Reference Catalog of Bright Galaxies* (Austin: University of Texas Press).
Edelson, R. A., and Malkan, M. A. 1986, *Ap. J.*, **308**, 59.
Elvis, M., and Lockman, F. J. 1988, in preparation.

Elvis, M., Maccacaro, T., Wilson, A. S., Ward, M. J., Penston, M. V., Fosbury, R. A. E., and Perola, G. C. 1978, *M.N.R.A.S.*, **183**, 129.
Elvis, M., Wilkes, B. J., and Tananbaum, H. 1985, *Ap. J.*, **292**, 357.
ESA (European Space Agency). 1984, *EXOSAT Observers Guide, Part III: The Final Observation Tape Handbook*, Rev. 2 (Noordwijk: ESA).
Fabbiano, G. 1988, *Ap. J.*, **325**, 544.
Fabbiano, G., and Trinchieri, G. 1984, *Ap. J.*, **286**, 491.
———. 1985, *Ap. J.*, **296**, 430.
———. 1987, *Ap. J.*, **315**, 46.
Ferland, G. J., and Osterbrock, D. E. 1986, *Ap. J.*, **300**, 658.
Giacconi, R., *et al.* 1979, *Ap. J.*, **230**, 540.
Gorenstein, P., Harnden, R. F., and Fabricant, D. 1981, *IEEE Trans. Nucl. Sci.*, **NS-28**, 869.
Harnden, F. R., Fabricant, D. G., Harris, D. E., and Schwarz, J. 1984, *Smithsonian Ap. Obs. Spec. Rept.*, No. 393.
Jenkins, E. B., and Savage, B. D. 1974, *Ap. J.*, **187**, 243.
Kallman, T., and Mushotzky, R. F. 1985, *Ap. J.*, **292**, 49.
Kriss, G. A., Canizares, C. R., and Ricker, G. 1980, *Ap. J.*, **242**, 492.
Krolik, J. H., and Begelman, M. 1986, *Ap. J. (Letters)*, **308**, L55.
Krolik, J. H., and Kallman, T. R. 1987, *Ap. J. (Letters)*, **320**, L5.
Krolik, J. H., McKee, C. F., and Tarter, C. B. 1981, *Ap. J.*, **249**, 422.
Lawrence, A. 1987, *Pub. A.S.P.*, **99**, 309.
Lawrence, A., and Elvis, M. 1982, *Ap. J.*, **256**, 410.
Lawrence, A., Walker, D., Rowan-Robinson, M., Leech, K. J., and Penston, M. V. 1986, *M.N.R.A.S.*, **219**, 687.
Lawrence, A., Watson, M. G., Pounds, K. A., and Elvis, M. 1987, *Nature*, **253**, 694.
Leech, K. J., Penston, M. V., Lawrence, A., Walker, D., and Rowan-Robinson, M. 1987, *M.N.R.A.S.*, submitted.
Maccacaro, T., Perola, G. C., and Elvis, M. 1982, *Ap. J.*, **257**, 47.
Makishima, K. 1986, *The Physics of Accretion onto Compact Objects, Lecture Notes in Phys.*, Vol. **266** (Berlin: Springer), p. 249.
Monier, R., and Halpern, J. P. 1987, *Ap. J. (Letters)*, **315**, L17.
Morrison, R., and McCammon, D. 1983, *Ap. J.*, **270**, 119.
Mushotzky, R. F., 1982, *Ap. J.*, **252**, 92.
Mushotzky, R. F. 1984, *Adv. Space Res.*, Vol. **3**, No. 10–12, p. 157.
Neugebauer, G., *et al.* 1980, *Ap. J.*, **238**, 502.
Norris, R. P., Baan, W. A., Haschick, W. D., Diamond, P. J., and Booth, R. S. 1985, *M.N.R.A.S.*, **213**, 821.
Norris, R. P. 1985, *M.N.R.A.S.*, **216**, 701.
Osborne, J. 1985, *EXOSAT Express*, No. 13, p. 42.
Osborne, J., and Angelini, L. 1986, *EXOSAT Express*, No. 17, p. 3.
Pounds, K. A., Stanger, V. J., Turner, T. J., King, A. R., and Czerny, B. 1987, *M.N.R.A.S.*, **224**, 443.
Raymond, J. 1980, private communication.
Raymond, J., and Smith, B. W. 1977, *Ap. J. Suppl.*, **35**, 419.
Rowan-Robinson, M. 1977, *Ap. J.*, **213**, 635.
Shakura, N. A., and Sunyaev, R. A. 1973, *Astr. Ap.*, **35**, 337.
Smith, A. 1984, *EXOSAT Express*, No. 5, p. 48.
Snijders, M. A. J., Netzer, H., and Boksenberg, A. 1986, *Ap. J.*, **222**, 549.
Soifer, B. T., Rice, W. L., Mould, J. R., Gillett, F. C., Rowan-Robinson, M., and Habing, H. J. 1986, *Ap. J.*, **304**, 651.
Taylor, B. G., Andersen, R. D., Peacock, A., and Zobl, R. 1981, *Space Sci. Rev.*, **30**, 479.
Tennant, A., and Mushotzky, R. F. 1983, *Ap. J.*, **264**, 92.
Watson, M. G., Stanger, V., and Griffiths, R. E. 1984, *Ap. J.*, **286**, 144.
Wilkes, B. J., and Elvis, M. 1987, *Ap. J.*, **323**, 243.
Willner, S. P. 1984, in *Galactic and Extragalactic Infrared Spectroscopy* ed. M. F. Kessler and J. P. Phillips (Dordrecht: Reidel), p. 37.
Wilson, A. S., and Ulvestad, J. S. 1983, *Ap. J.*, **275**, 8.
Wood, K. S., *et al.* 1984, *Ap. J. Suppl.*, **56**, 507.

MARTIN ELVIS: Harvard-Smithsonian Center for Astrophysics, 60 Garden Street, Cambridge, MA 02138

ANDREW LAWRENCE: School of Mathematical Sciences, Queen Mary College, University of London, Mile End Road, London E1 4NS, England